Article

SOURCE DATA | TRANSPARENT PROCESS

THE EMBO JOURNAL

LAPTM4B is a PtdIns(4,5)P_2 effector that regulates EGFR signaling, lysosomal sorting, and degradation

Xiaojun Tan, Yue Sun, Narendra Thapa, Yihan Liao, Andrew C Hedman & Richard A Anderson*

Abstract

Lysosomal degradation is essential for the termination of EGF-stimulated EGF receptor (EGFR) signaling. This requires EGFR sorting to the intraluminal vesicles (ILVs) of multi-vesicular endosomes (MVEs). Cytosolic proteins including the ESCRT machineries are key regulators of EGFR intraluminal sorting, but roles for endosomal transmembrane proteins in receptor sorting are poorly defined. Here, we show that LAPTM4B, an endosomal transmembrane oncoprotein, inhibits EGF-induced EGFR intraluminal sorting and lysosomal degradation, leading to enhanced and prolonged EGFR signaling. LAPTM4B blocks EGFR sorting by promoting ubiquitination of Hrs (an ESCRT-0 subunit), which inhibits the Hrs association with ubiquitinated EGFR. This is counteracted by the endosomal PIP kinase, PIPKIγi5, which directly binds LAPTM4B and neutralizes the inhibitory function of LAPTM4B in EGFR sorting by generating PtdIns(4,5)P_2 and recruiting SNX5. PtdIns(4,5)P_2 and SNX5 function together to protect Hrs from ubiquitination, thereby promoting EGFR intraluminal sorting. These results reveal an essential layer of EGFR trafficking regulated by LAPTM4B, PtdIns(4,5)P_2 signaling, and the ESCRT complex and define a mechanism by which the oncoprotein LAPTM4B can transform cells and promote tumor progression.

Keywords EGFR; LAPTM4B; PIPKIγi5; PtdIns(4,5)P_2
Subject Categories Membrane & Intracellular Transport; Signal Transduction
DOI 10.15252/embj.201489425 | Received 10 July 2014 | Revised 11 December 2014 | Accepted 12 December 2014 | Published online 14 January 2015
The EMBO Journal (2015) 34: 475–490

Introduction

Epidermal growth factor receptor (EGFR) plays fundamental roles not only in physiological cellular processes, but also in diseases such as cardiovascular hypertrophy and cancers (Kagiyama *et al*, 2002; Eguchi *et al*, 2003; Mendelsohn & Baselga, 2006). Therefore, EGFR expression levels and signaling strength must be tightly controlled. One key mechanism to downregulate EGFR signaling is the lysosomal trafficking and degradation of the activated receptor. Upon ligand binding, activated EGFR is rapidly internalized to endosomes, where ligand-bound EGFR continues to signal until it is sorted to intraluminal vesicles (ILVs) in the multi-vesicular endosomes (MVEs) or late endosomes (Wiley, 2003; Sorkin & Goh, 2008). Finally, the MVE fuses with the lysosome, resulting in EGFR degradation (Eden *et al*, 2009).

Intraluminal sorting of EGFR is an essential step that terminates EGFR signaling, which is mediated by the endosomal sorting complex required for transport (ESCRT) machineries (Williams & Urbé, 2007; Raiborg & Stenmark, 2009; Henne *et al*, 2011). The ESCRT-mediated EGFR ILV sorting pathway requires ubiquitination of EGFR (Williams & Urbé, 2007). Upstream ESCRT subunits, including Hrs and TSG101, contain ubiquitin-interacting motifs (UIM) that recognize ubiquitinated EGFR, and cooperate with downstream ESCRT complexes for EGFR ILV sorting (Raiborg & Stenmark, 2009). Hrs, like other ESCRT subunits, is a cytosolic protein that is recruited to the endosome by phosphoinositides and protein–protein interactions (Di Paolo & De Camilli, 2006; Lindmo & Stenmark, 2006; Henne *et al*, 2013). The function of Hrs is also regulated by the E3 ubiquitin ligases Nedd4-1 and Nedd4-2 that ubiquitinate Hrs and trigger an intramolecular interaction between the Hrs-UIM and ubiquitin (Katz *et al*, 2002; Hoeller *et al*, 2006; Persaud *et al*, 2009). This interaction inhibits Hrs function by preventing it from binding to ubiquitinated cargos, like EGFR.

Phosphatidylinositol 4,5-bisphosphate (PtdIns(4,5)P_2) is a lipid messenger that regulates many cellular processes, including actin and focal adhesion dynamics, endocytosis, exocytosis, and gene expression (Anderson & Marchesi, 1985; Ling *et al*, 2002; Mellman *et al*, 2008; Thapa *et al*, 2012; Balla, 2013; Sun *et al*, 2013c). PtdIns(4,5)P_2 has been traditionally thought to be largely at the plasma membrane (Di Paolo & De Camilli, 2006), but a broader intracellular distribution and synthesis have been recently revealed (Sun *et al*, 2013c). Type I phosphatidylinositol-4-phosphate (PIP) 5-kinases (PIPKIα, β, and γ) are the major enzymes for PtdIns(4,5)P_2 generation in cells (Heck *et al*, 2007). PIPKI has critical functions in various protein trafficking processes, including endocytosis, exocytosis, and endosomal trafficking (Bairstow *et al*, 2006; Schramp *et al*, 2012; Thapa *et al*, 2012; Sun *et al*, 2013a,b). There are six splice variants of human PIPKIγ (i1-i6), each with distinct C-terminal extensions that mediate specific protein–protein interactions, leading to distinct intracellular targeting of each isoform (Schill & Anderson, 2009; Xia *et al*, 2011). PIPKIγi5 is targeted to endosomes and generates phosphoinositide signals that control EGFR intraluminal

Program in Molecular and Cellular Pharmacology, University of Wisconsin–Madison, School of Medicine and Public Health, Madison, WI, USA
*Corresponding author. Tel: +1 608 262 7436; E-mail: raanders@wisc.edu

sorting (Sun *et al*, 2013b). This pathway requires an interaction between PIPKIγi5 and sorting nexin 5 (SNX5). PIPKIγi5 and its kinase activity regulate the interaction of SNX5 with Hrs to protect Hrs from ubiquitination and promote the Hrs association with EGFR. Thus, PIPKIγi5, its kinase activity, and SNX5 control Hrs function in EGFR intraluminal sorting and degradation (Sun *et al*, 2013b).

All the ESCRT subunits including Hrs are cytosolic proteins recruited to endosomal surface during ILV sorting. The roles for resident endosomal transmembrane proteins in the regulation of ESCRT complexes and ILV sorting are poorly defined. A family of the resident proteins is the mammalian lysosomal-associated protein transmembrane (LAPTM) that has three members, LAPTM4A, LAPTM4B, and LAPTM5, with ~36% sequence similarities. All LAPTMs are multi-transmembrane proteins primarily localized to the late endosome/lysosome (Adra *et al*, 1996; Hogue *et al*, 2002; Shao *et al*, 2003; Pak *et al*, 2006; Milkereit & Rotin, 2011). LAPTM4B has four transmembrane domains, with two cytoplasmic termini (Shao *et al*, 2003). LAPTM4B is upregulated in a wide variety of human cancers, including breast, liver, lung, colon, uterine, and ovarian cancers (Shao *et al*, 2003; Kasper *et al*, 2005; Li *et al*, 2010b). LAPTM4B overexpression in cancers correlates with poor prognosis (Yang *et al*, 2010b; Kang *et al*, 2012). Further, ectopic expression of LAPTM4B induces transformation and tumorigenesis of normal human cells (Li *et al*, 2011) and promotes proliferation and migration of cancer cells *in vitro* and *in vivo* (Yang *et al*, 2010a). The underlying mechanisms for the LAPTM4B oncogenesis are not defined, but LAPTM4B overexpression enhances AKT activation (Li *et al*, 2010a).

Here, we report that LAPTM4B blocks EGF-stimulated EGFR intraluminal sorting and degradation. In this pathway, LAPTM4B binds to PIPKIγi5 and its product PtdIns(4,5)P_2, and this neutralizes LAPTM4B inhibition of EGFR trafficking. These results reveal an essential layer of EGFR trafficking regulated by LAPTM4B and phosphoinositide signaling and may represent the underlying mechanism for LAPTM4B oncogenesis.

Results

PIPKIγi5 interacts with endosomal transmembrane protein LAPTM4B

The endosomal PIP kinase, PIPKIγi5, generates the lipid messenger PtdIns(4,5)P_2 and is required for EGFR intraluminal sorting and degradation (Sun *et al*, 2013b). Based on a yeast two-hybrid screen using the C-terminal 223 amino acids of PIPKIγi5 as bait (Sun *et al*, 2013b), the lysosomal-associated protein Transmembrane 4B (LAPTM4B) was identified as a PIPKIγi5 interactor. The interaction between endogenous LAPTM4B and PIPKIγi5 was confirmed by co-immunoprecipitation (co-IP) (Fig 1A). This is a specific interaction, as among the three LAPTM family members, PIPKIγi5 specifically associated with LAPTM4B (Fig 1B). The LAPTM4B interaction is also specific for PIPKIγi5, but not other PIPKIγ isoforms (Fig 1C). To test whether the kinase activity of PIPKIγi5 modulates its LAPTM4B interaction, a D316A kinase dead mutant (PIPKIγi5KD) was used in co-IP assays. As shown in Fig 1D, PIPKIγi5KD had diminished LAPTM4B association, indicating that phosphoinositide generation is required. PIPKIγi5 modulates EGF-stimulated EGFR lysosomal trafficking, but the PIPKIγi5–LAPTM4B interaction was not regulated by EGF stimulation (Fig 1D).

Ectopically expressed LAPTM4B localizes to late endosomes and lysosomes (Milkereit & Rotin, 2011; Vergarajauregui *et al*, 2011). Consistently, we observed that HA-tagged LAPTM4B was primarily colocalized with late endosome/lysosome markers CD63 and LAMP1 and a partial overlap with early endosome marker EEA1 (Supplementary Fig S1A). To ascertain the subcellular localization of the endogenous protein, rabbit polyclonal LAPTM4B anti-sera were used to stain cells. The anti-sera stained endogenous LAPTM4B with significant colocalization with both LAMP1 and EEA1 (Fig 1E and F), indicating a wide distribution of LAPTM4B through the endosomal system (Fig 1G). The specificity of the LAPTM4B anti-sera staining was validated by LAPTM4B knockdown that eliminated the endosomal but not the nuclear staining

Figure 1. PIPKIγi5 specifically interacts with the endosomal transmembrane protein LAPTM4B.

A Endogenous PIPKIγi5 and LAPTM4B were immunoprecipitated from the whole-cell lysates of MDA-MB-231 cells followed by immunoblotting to examine the co-immunoprecipitated PIPKIγi5 and LAPTM4B.

B PIPKIγi5 specifically interacts with LAPTM4B, but not LAPTM4A or LAPTM5. Top: schematic diagram of all three LAPTM members. Bottom: each Flag-tagged LAPTM protein was immunoprecipitated from HEK293 cells cotransfected with Myc-tagged PIPKIγi5 and empty vector or Flag-tagged LAPTM, and the co-immunoprecipitated PIPKIγi5 was examined by immunoblotting.

C LAPTM4B selectively associates with PIPKIγi5. Top: schematic diagram of four PIPKI isoforms. Bottom: Myc-tagged PIPKIγi5 was immunoprecipitated from HEK293 cells expressing Flag-tagged LAPTM4B and each isoform of PIPKI, followed by immunoblotting to examine the co-immunoprecipitated LAPTM4B.

D Kinase activity of PIPKIγi5 is required for LAPTM4B association. HEK293 cells expressing LAPTM4B and wild-type (WT) or kinase-dead (KD) PIPKIγi5 were starved overnight, stimulated or not with 100 ng/ml EGF for 15 min, and harvested for immunoprecipitation with anti-myc. The co-immunoprecipitated LAPTM4B was detected by immunoblotting.

E Endogenous LAPTM4B is targeted to both early and late endosomes. MDA-MB-231 cells were fixed and costained for endogenous LAPTM4B (red) and EEA1 or LAMP1 (green). Boxes are selected regions for magnified view. Note: non-specific nuclear staining by the LAPTM4B anti-sera. Scale bar: 10 μm.

F Quantification of LAPTM4B colocalization with EEA1 and LAMP1 (mean + SD; $n \geq 4$).

G Schematic diagram for LAPTM4B endosomal localization based on quantification in (F).

H LAPTM4B partially colocalizes with PIPKIγi5. MDA-MB-231 cells expressing Myc-tagged PIPKIγi5 were stained with LAPTM4B anti-sera (red), anti-Myc (green), and DAPI. Box is selected region for magnified view. Scale bar: 10 μm.

I MDA-MB-231 cells stably expressing Flag-LAPTM4B were stained with LAPTM4B anti-sera followed by silver-enhanced immuno-electron microscopy. The early and late MVEs were defined by the number of intraluminal vesicles. N, nucleus; M, mitochondria; MVE, multi-vesicular endosome; and PM, plasma membrane. Scale bars: 2 μm (left); 200 nm (middle and right).

Data information: Data are representative for at least four independent experiments. IP, immunoprecipitate; WCL, whole-cell lysates.
Source data are available online for this figure.

(Supplementary Fig S1B and C). LAPTM4B knockdown did not change LAPTM5 staining (Supplementary Fig S1B), indicating that both the LAPTM4B siRNA and anti-sera are specific. To determine whether LAPTM4B and PIPKIγi5 colocalize in cells, Myc-tagged PIPKIγi5 was expressed and costained with endogenous LAPTM4B. As shown in Fig 1H, PIPKIγi5 was localized to subdomains of

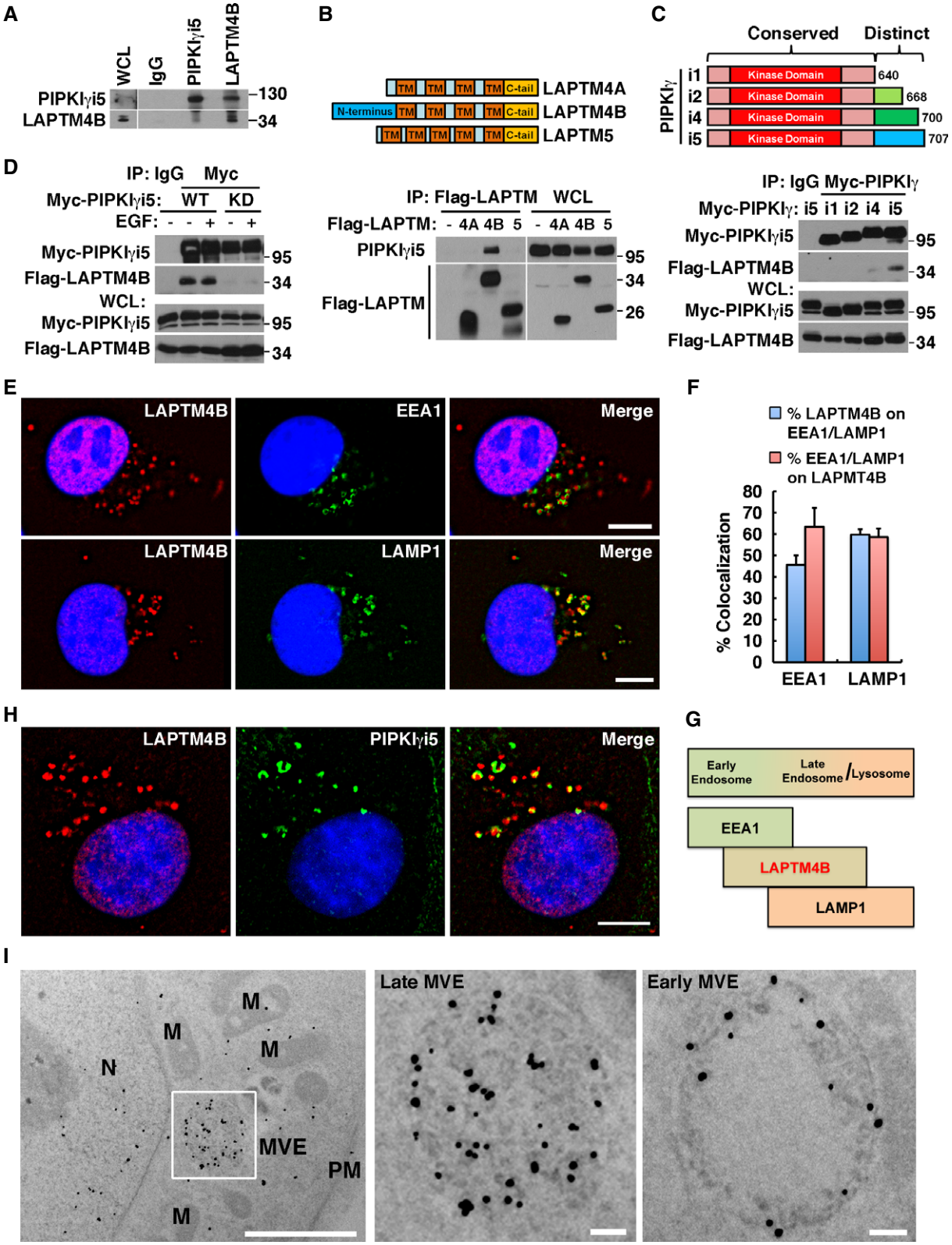

Figure 1.

LAPTM4B-positive endosomes. Loss of LAPTM4B did not prevent endosomal targeting of PIPKIγi5 (Supplementary Fig S1C), consistent with additional PIPKIγi5 targeting factors at endosomes.

As LAPTM4B is a transmembrane protein at endosomes, we examined whether LAPTM4B is targeted to both endosomal limiting membrane and intraluminal vesicles by silver-enhanced immuno-electron microscopy (immuno-EM) that detects the subendosomal localization of LAPTM4B. As shown in Fig 1I, LAPTM4B specifically accumulated at MVEs, on both the limiting membrane and intraluminal vesicles. Early MVEs have fewer ILVs, and LAPTM4B was primarily at the limiting membrane (Fig 1I, right). These data support that LAPTM4B is initially sorted to the limiting membrane of MVEs and then partially sorted onto ILVs as the MVE matures. This is consistent with a partial colocalization between LAPTM4B and PIPKIγi5 at endosome surfaces.

LAPTM4B inhibits EGF-stimulated EGFR degradation

PIPKIγi5 plays a key role in ESCRT-mediated EGFR ILV sorting and lysosomal degradation (Sun *et al*, 2013b). As LAPTM4B interacts with PIPKIγi5 (Fig 1), we explored whether LAPTM4B also regulates EGF-stimulated EGFR degradation. Endogenous LAPTM4B expression was knocked down by siRNA in MDA-MB-231 cells. Strikingly, the degradation rate of EGFR was significantly enhanced after LAPTM4B knockdown (Fig 2A and B). After 1 h of EGF stimulation, the EGFR levels in control cells were not significantly reduced, but half of the EGFR was degraded in LAPTM4B knockdown cells (Fig 2A and B). Accelerated EGFR degradation after LAPTM4B knockdown also reduced EGFR and AKT signaling (Fig 2A, C and D). Knockdown of LAPTM4B in A431 cells (Supplementary Fig S2A) resulted in even more dramatic acceleration of EGFR degradation (Supplementary Fig S2B, CQ- and C), indicating that this was not a cell type-specific result. Pretreatment with the lysosomal inhibitor chloroquine fully blocked EGFR degradation in MDA-MB-231 and A431 cells pretreated with either control or LAPTM4B siRNA (Supplementary Fig S2B, CQ + and D), indicating that the EGFR degradation in LAPTM4B knockdown cells remains lysosomal mediated. A distinct siRNA (siLAPTM4B#2) also efficiently knocked down LAPTM4B expression (Supplementary Fig S2E) and accelerated EGFR degradation (Supplementary Fig S2F and G).

To further confirm that loss of LAPTM4B accelerates EGF-stimulated EGFR degradation, a pulse-chase experiment using Alexa-555-EGF was performed to analyze EGF degradation in control or LAPTM4B knockdown cells by fluorescence microscopy (Fig 2E). After a brief pulse with a lower concentration of Alexa-555-EGF, only a small pool (~10%) of total EGFR is EGF-bound and internalized (Fig 2F). Though similar amounts of EGF were initially internalized in control and LAPTM4B knockdown cells, the loss of EGF was more rapid in cells lacking LAPTM4B (Fig 2E and G). The combined results confirm that LAPTM4B inhibits EGF-stimulated EGFR degradation and enhances EGFR signaling.

LAPTM4B is overexpressed in many human cancers (Kasper *et al*, 2005; Li *et al*, 2010b). Therefore, we investigated whether ectopic expression of LAPTM4B could inhibit EGFR degradation. As shown in Fig 2H–K, overexpression of LAPTM4B strongly inhibited EGF-stimulated EGFR degradation, resulting in greatly enhanced and prolonged activation of EGFR and AKT.

LAPTM4B inhibits EGFR trafficking through late endosomes

LAPTM4B is an endosomal protein suggesting that it may inhibit EGFR degradation by modulating EGFR endosomal trafficking. Cells were stimulated with EGF, and EGFR was costained with EEA1 and LAMP1, respectively. Trafficking of EGFR through these compartments was analyzed by quantifying the colocalization of EGFR with EEA1 or LAMP1. After 15 min, the majority of EGFR accumulated at EEA1 compartments in both control and LAPTM4B knockdown cells (Fig 3A and B), signifying that internalization and trafficking to the early endosome were not affected. After 2 h, EGFR colocalized well with LAMP1 in control cells but surprisingly not in LAPTM4B knockdown cells where EGFR showed more colocalization with EEA1 [Fig 3A–D, chloroquine (−)]. It is important to note that EGFR degradation is more rapid in LAPTM4B knockdown cells compared to control cells (Fig 2); the decreased EGFR colocalization with LAMP1 may result from accelerated lysosomal delivery and degradation of EGFR in knockdown cells, but not a block of EGFR trafficking at the early endosome. To confirm this possibility, the EGFR trafficking assay was performed in cells pretreated with lysosomal inhibitor chloroquine to block EGFR degradation. As shown in Fig 3A–D, chloroquine pretreatment rescued EGFR colocalization with LAMP1 in LAPTM4B knockdown cells and decreased EGFR colocalization with EEA1. These combined results indicate that EGFR is delivered faster into lysosomes for degradation upon loss of LAPTM4B.

In cells, LAPTM4B is stochastically expressed with some cells having high and others low LAPTM4B levels (Fig 3E, see arrows). To determine whether EGF-stimulated EGFR trafficking is slowed in LAPTM4B-positive late endosomes, cells were stimulated with EGF for 15 min or 120 min and then fixed and costained for endogenous LAPTM4B and EGFR. After 15 min of EGF stimulation, all cells had similar amounts of EGFR staining at endosomes with partial colocalization with LAPTM4B (Fig 3E, top). After 120 min of EGF stimulation, significantly more EGFR was detected in cells with higher LAPTM4B expression (arrows), and the remaining EGFR colocalized with LAPTM4B (Fig 3E, bottom). These results indicate that EGF-stimulated EGFR trafficking is inhibited in LAPTM4B-positive endosomes. The scatter plot of the EGFR versus LAPTM4B levels in each cell at 15 min and 120 min, respectively, was shown in Fig 3F; no significant correlation between EGFR and LAPTM4B levels at 15 min was detected, but a positive correlation was observed at 120 min, consistent with the model that enhanced LAPTM4B expression inhibits EGFR degradation.

LAPTM4B inhibits EGF-stimulated EGFR intraluminal sorting

LAPTM4B may enhance EGFR signaling by inhibiting EGF-stimulated EGFR intraluminal sorting in LAPTM4B-positive endosomes. For this, intraluminal sorting of Alexa-555-EGF into enlarged endosomes induced by expression of constitutively active Rab5Q79L was quantified (Stenmark *et al*, 1994; Simonsen *et al*, 1998; Hanafusa *et al*, 2011). The results demonstrate diminished intraluminal sorting of EGF occurred at endosomes with higher LAPTM4B staining (Fig 4A). Quantification of EGF intraluminal sorting revealed a significant inverse relationship between the EGF intraluminal sorting and LAPTM4B levels at individual endosomes

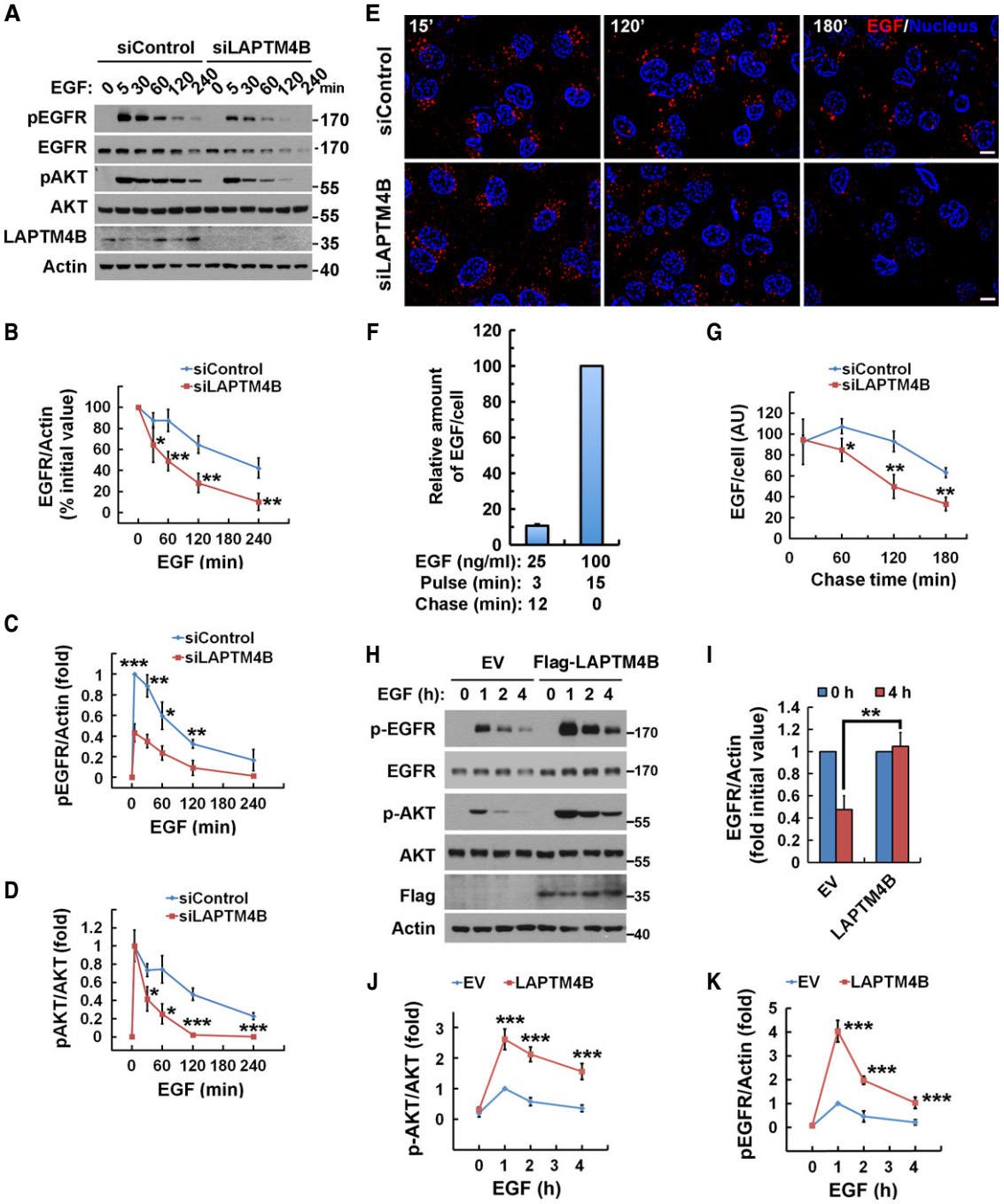

Figure 2. LAPTM4B knockdown accelerates EGF-stimulated EGFR degradation.

A MDA-MB-231 cells transfected with control or LAPTM4B siRNA were starved and stimulated with 100 ng/ml EGF for indicated time periods, followed by whole-cell lysate harvest for immunoblotting analysis of EGFR levels.

B–D Quantification of the levels of EGFR (B), pEGFR (Y1068)(C), and pAKT (S473)(D) from the analysis in (A) (mean ± SD; n = 3).

E Control or LAPTM4B siRNA-transfected MDA-MB-231 cells were starved, pulsed with 25 ng/ml Alexa-555-EGF for 3 min, washed, and chased for indicated time periods followed by fixation, DAPI staining, and fluorescence microscopy. Scale bar: 10 μm.

F Quantification of the relative amounts of Alexa-555-EGF internalized in the indicated conditions (mean + SD, n = 3).

G Quantification of the Alexa-555-EGF degradation in control and LAPTM4B knockdown cells in (E) (mean ± SD, n = 3).

H Control or LAPTM4B-overexpressing MDA-MB-231 cells were starved and then stimulated with 100 ng/ml EGF for 1–4 h. EGFR degradation and signaling were analyzed by Western blot. Specific antibodies recognizing pEGFR (Y1068) and pAKT (S473) were used.

I–K Quantification for the levels of EGFR (I) and pEGFR (J) normalized to actin and pAKT (K) normalized to AKT in control or LAPTM4B-overexpressing cells (mean ± SD, n = 3).

Data information: Data are representative for at least three independent experiments. *P < 0.05, **P < 0.01, ***P < 0.001, one-tailed t-test.
Source data are available online for this figure.

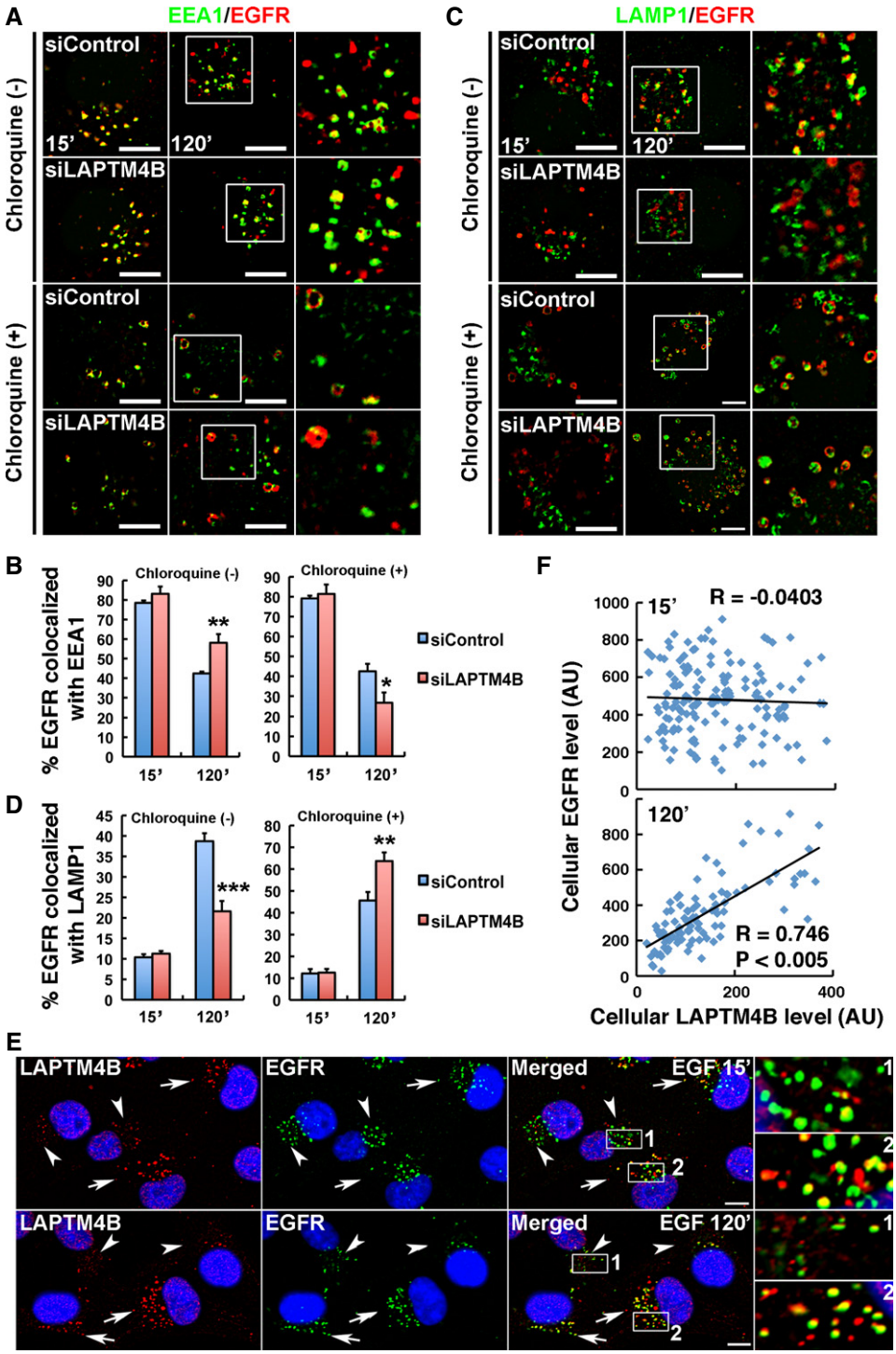

Figure 3. LAPTM4B inhibits EGF-stimulated EGFR endosomal sorting.

A–D Control or LAPTM4B siRNA-transfected MDA-MB-231 cells were starved, pretreated or not with chloroquine for 2 h, stimulated with 100 ng/ml EGF for 15 min, washed, and chased for indicated time periods before fixation for costaining of EGFR (red) with EEA1 (A, green) or LAMP1 (C, green). Quantification of the average percentages of EGFR signals colocalized with EEA1 (B) and LAMP1 (D) at indicated time points; mean + SD; $n = 3$; $^{*}P < 0.05$, $^{**}P < 0.01$, $^{***}P < 0.001$, one-tailed *t*-test.

E MDA-MB-231 cells were starved, stimulated with 100 ng/ml EGF for 15 or 120 min, fixed, and costained for EGFR and LAPTM4B, followed by fluorescence microscopy. Cells with higher and lower LAPTM4B expression were marked with arrows and arrowheads, respectively.

F The amounts of total EGFR staining in individual cells in (E) were plotted against LAPTM4B levels at 15 min and 120 min, respectively. Note: for LAPTM4B quantification, the non-specific nuclear staining was not included. Trend lines and Pearson's correlation coefficients are shown. AU, arbitrary unit.

Data information: Data are representative for three independent experiments. Boxes are selected regions for magnified view. Scale bars: 10 μm.

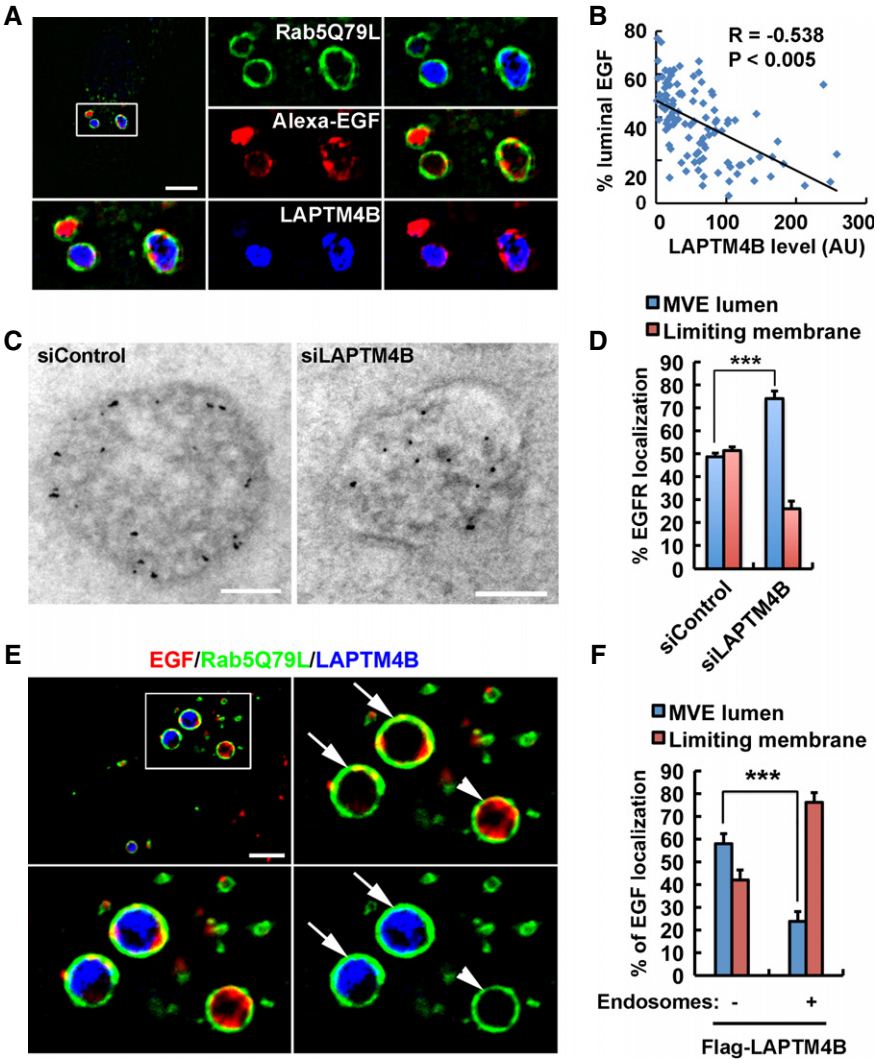

Figure 4. LAPTM4B inhibits EGF-stimulated intraluminal sorting of EGFR.

A MDA-MB-231 cells expressing GFP-Rab5Q79L were starved and stimulated with 100 ng/ml Alexa-555-EGF for 90 min followed by fixation and immunostaining for LAPTM4B (blue).

B The percentages of luminal Alexa-555-EGF in individual endosomes were plotted against endosomal LAPTM4B levels. Trend lines and Pearson's correlation coefficients are shown. Data are representative for three independent experiments.

C Control or LAPTM4B knockdown MDA-MB-231 cells were starved overnight, cell surface EGFR was labeled with immuno-gold on ice. Cells were then stimulated with EGF for 1 h at 37°C and fixed for the EM study. Scale bar, 200 nm. See Materials and Methods for details.

D Relative amounts of immuno-gold-labeled EGFR in the MVE lumen versus MVE limiting membrane were quantified. Over 80 endosomes for each siRNA treatment from three independent experiments were used for quantification (mean + SD; ***$P < 0.001$, one-tailed t-test).

E MDA-MB-231 cells were transfected with GFP-Rab5Q79L and Flag-LAPTM4B, starved, and stimulated with Alexa-555-EGF for 90 min and followed by intraluminal sorting analysis. See Materials and Methods for details.

F Quantification of EGF localization in LAPTM4B-positive and LAPTM4B-negative endosomes in (E) (mean + SD; $n = 3$; ***$P < 0.0007$, one-tailed t-test).

Data information: Boxes are selected regions for magnified view. Scale bars (A, E): 10 μm.

(Fig 4B), suggesting that LAPTM4B inhibits intraluminal sorting of EGF at LAPTM4B-positive endosomes.

To confirm the role for LAPTM4B in EGFR intraluminal sorting, an EM approach was used. Serum-starved cells were stimulated with 100 ng/ml EGF for 1 h, and the intraluminal sorting of immuno-gold labeled EGFR was quantified. Knockdown of LAPTM4B significantly increases EGF-stimulated intraluminal sorting of EGFR from ~50% in control cells to ~75% in knockdown cells (Fig 4C and D). When overexpressed, LAPTM4B displayed a non-uniform distribution among endosomes, and consistently, intraluminal sorting of Alexa-555-EGF was strongly inhibited in LAPTM4B-positive endosomes (Fig 4E and F). Together, these results demonstrate that LAPTM4B blocks EGF-stimulated EGFR intraluminal sorting in LAPTM4B-positive endosomes.

As LAPTM4B inhibits EGFR intraluminal sorting, the EGFR accumulated on the endosomal surface could be recycled (Sorkin *et al*, 1991). To assess this, EGFR recycling assay was performed in control and LAPTM4B knockdown cells (Sigismund *et al*, 2008). Surprisingly,

knockdown of LAPTM4B did not change EGF-stimulated EGFR recycling (Supplementary Fig S3). These results indicate that LAPTM4B-promoted EGFR signaling comes from active EGFR at the endosome as LAPTM4B blocks EGFR intraluminal sorting at LAPTM4B-positive endosomes without enhancing EGFR recycling.

PtdIns(4,5)P_2 regulates LAPTM4B interaction with PIPKIγi5

To examine how the LAPTM4B–PIPKIγi5 interaction may modulate EGFR trafficking and degradation, the interaction was further characterized. LAPTM4B is a unique member of the LAPTM family as it has an additional N-terminal extension (amino acids 1–91) (Shao *et al*, 2003). It has been shown that the pro-survival functions of human LAPTM4B require its N-terminal extension (Shao *et al*, 2003). Deletion of the LAPTM4B N-terminus abolished the interaction with PIPKIγi5 (Fig 5A), and the LAPTM4B N-terminus (LAPTM4B-N) directly interacted with PIPKIγi5 C-terminus in GST pull-down assay (Fig 5B). Further, co-IP experiments using LAPTM4B truncation mutants revealed that amino acids 1–40 were not critical for PIPKIγi5 interaction (Fig 5C), indicating that amino acids 41–91 were required. This region contains a polybasic motif (PBM) with a cluster of basic arginine residues (Fig 5D). The cytoplasmic PBMs in ion channels and transporters have been shown to bind PtdIns(4,5)P_2, which is essential for their functions (Suh & Hille, 2005; Huang, 2007). To analyze whether the LAPTM4B-PBM binds phosphoinositides, the LAPTM4B-N with or without PBM mutation (6RQ and 8RQ, Fig 5D) was expressed and purified from *E. coli* and assayed for phosphoinositide binding using PIP strips (Fig 5E). Wild-type LAPTM4B-N bound multiple phosphoinositides including PtdIns(4,5)P_2, while the 6RQ and 8RQ mutants lost all phosphoinositide binding ability (Fig 5F), indicating that the LAPTM4B-PBM is capable of binding to phosphoinositides.

In GST pull-down assays, wild-type LAPTM4B-N and the 6RQ mutant interacted with PIPKIγi5 equally well (Fig 5G), indicating that the mutated residues are not direct PIPKIγi5 binding sites. However, although the 6RQ mutant retained wild-type subcellular localization (Supplementary Fig S4A), it had reduced interaction with PIPKIγi5 in co-IP (Fig 5H, lanes 2 and 4), suggesting PtdIns(4,5)P_2 regulation of the interaction in cells. Consistently, PIPKIγi5KD that does not generate PtdIns(4,5)P_2 had diminished LAPTM4B association (Fig 1D). Additionally, while the wild-type PIPKIγi5 associates with wild-type LAPTM4B much more strongly than with PBM mutants (Fig 5H, lanes 2–4), the PIPKIγi5KD interacts equally with wild-type and PBM-mutated LAPTM4B (Fig 5H, lanes 5–7). These data signify that *in vivo* the LAPTM4B–PIPKIγi5 interaction is regulated by PtdIns(4,5)P_2 generated by PIPKIγi5.

To directly determine whether PtdIns(4,5)P_2 regulates the LAPTM4B–PIPKIγi5 interaction, a GST pull-down experiment with or without PtdIns(4,5)P_2 was performed. This revealed that PtdIns(4,5)P_2 dose-dependently enhanced LAPTM4B binding to PIPKIγi5 (Fig 5I). Although other phosphoinositides including PtdIns(3)P, PtdIns(4)P, and PtdIns(3,5)P_2 bound LAPTM4B-N in both PIP strips assays (Fig 5F) and liposome-binding assays (Fig 5J), yet regulation of the LAPTM4B–PIPKIγi5 interaction was PtdIns(4,5)P_2 specific (Fig 5K), consistent with regulation by PIPKIγi5 that generates PtdIns(4,5)P_2.

The binding between PIPKIγi5 and the 6RQ mutant of LAPTM4B is no longer stimulated by PtdIns(4,5)P_2 addition (Fig 5L), consistent with the loss of phosphoinositide binding for the 6RQ mutant (Fig 5F). The GST pull-down experiments were performed in the presence of PtdIns(4,5)P_2 in incubation buffer, but not washing buffer. To assess whether washing the pull-down complex with detergent removed PtdIns(4,5)P_2 from the complex, PtdIns(4,5)P_2 was added to the washing buffer to protect the protein–lipid complex. This addition did not further enhance the PtdIns(4,5)P_2-stimulated interaction between LAPTM4B and PIPKIγi5 (Supplementary Fig S4B), indicating that detergent wash did not disrupt the pull-down complex. Together, these results indicate that PtdIns(4,5)P_2, the product of PIPKIγi5, specifically regulates the interaction between LAPTM4B and PIPKIγi5.

Phosphoinositide binding inhibits the role of LAPTM4B in Hrs ubiquitination and EGFR degradation

For intraluminal sorting, activated EGFR is ubiquitinated and recognized by the ESCRT-0 subunit Hrs that sequesters EGFR and

Figure 5. Phosphoinositide regulates LAPTM4B interaction with PIPKIγi5.

A Co-immunoprecipitation (co-IP) of full-length or N-terminus-deleted LAPTM4B with PIPKIγi5 in HEK293 cells.
B GST-tagged LAPTM4B N-terminus (93 amino acids) and T7-tagged PIPKIγi5 C-terminus (223 amino acids) were purified from *E. coli* for *in vitro* GST pull-down assay.
C Co-IP of full-length or N-terminal deletion mutants of LAPTM4B with PIPKIγi5 in HEK293 cells. Δ25: amino acids 1–25 deleted.
D Schematic diagram of LAPTM4B with polybasic motif (PBM) magnified and PBM mutants specified.
E Coomassie Brilliant Blue staining of purified wild-type and mutated LAPTM4B N-termini.
F Purified LAPTM4B N-termini from (E) were used in PIP strips assay. LPA, lysophosphatidic acid; LPC, lysophosphocholine; PE, phosphatidylethanolamine; PC, phosphatidylcholine; S1P, sphingosine 1-phosphate; PI3,4,5P3, PtdIns(3,4,5)P_3, phosphatidylinositol (3,4,5)-trisphosphate; PA, phosphatidic acid; PS, phosphatidylserine.
G GST pull-down assay of wild-type or 6RQ mutant of LAPTM4B N-termini with PIPKIγi5 C-terminus.
H Co-IP of wild-type or PMB-mutated LAPTM4B with wild-type or kinase dead PIPKIγi5 in HEK293 cells.
I Top: GST pull-down assay of LAPTM4B N-terminus and PIPKIγi5 C-terminus with increased concentration of PtdIns(4,5)P_2 addition. Bottom: Quantification of the relative amounts of PIPKIγi5 C-terminus bound to LAPTM4B N-terminus in top panel (mean ± SD; n = 4).
J LAPTM4B N-terminus binds multiple phosphoinositides including PtdIns(4,5)P_2 in liposome-binding assay.
K Top: GST pull-down assay of LAPTM4B N-terminus and PIPKIγi5 C-terminus with 0.5 μM addition of different phosphoinositides. Bottom: Quantification of the relative amounts of PIPKIγi5 C-terminus bound to LAPTM4B N-terminus in top panel (mean + SD; n = 4).
L Top: GST pull-down assay of wild-type or 6RQ mutant of LAPTM4B N-terminus and PIPKIγi5 C-terminus with 0.5 μM addition of PtdIns(4,5)P_2. Bottom: Quantification of the relative amounts of PIPKIγi5 C-terminus bound to LAPTM4B N-terminus in top panel (mean + SD; n = 4).

Data information: Data are representative from at least three independent experiments; L4B, LAPTM4B; L4B-N, LAPTM4B N-terminus; Iγi5-CT, PIPKIγi5 C-terminus; PI, PtdIns, phosphatidylinositol; PI3P, PtdIns(3)P, phosphatidylinositol (3)-phosphate; PI4,5P2, PtdIns(4,5)P_2, phosphatidylinositol (4,5)-bisphosphate.
Source data are available online for this figure.

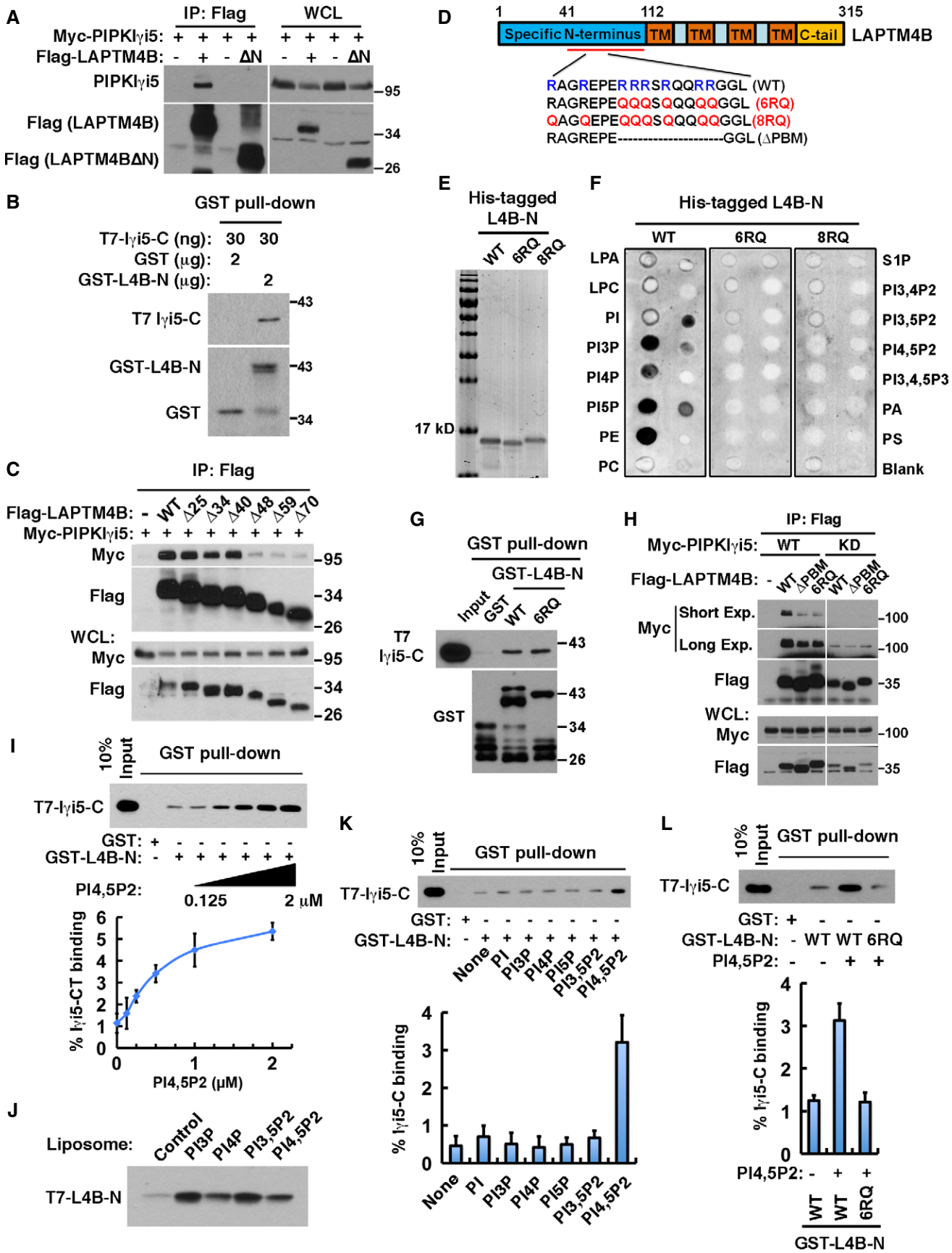

Figure 5.

recruits downstream ESCRT complexes (Raiborg *et al*, 2002; Raiborg & Stenmark, 2009; Sorkin & von Zastrow, 2009). To explore the mechanism by which LAPTM4B inhibits EGFR intraluminal sorting, we examined how LAPTM4B impacts the association between EGFR and Hrs. Loss of LAPTM4B enhanced the EGFR interaction with Hrs (Fig 6A), consistent with the enhanced EGFR intraluminal sorting and degradation in knockdown cells. This suggests that LAPTM4B may inhibit EGFR ILV sorting by blocking EGFR interaction with Hrs.

The interaction of EGFR with Hrs is dependent on the ubiquitination of EGFR (Eden *et al*, 2012), but loss of LAPTM4B did not affect EGFR ubiquitination (Supplementary Fig S5A). Ubiquitination of Hrs induces an intramolecular interaction between the Hrs-UIM and ubiquitin that inhibits Hrs interaction with ubiquitinated EGFR (Hoeller *et al*, 2006). Therefore, whether LAPTM4B regulates the ubiquitination of Hrs was determined. Loss of LAPTM4B diminished Hrs ubiquitination (Fig 6B), while overexpression of LAPTM4B enhanced Hrs ubiquitination (Fig 6C and D). Consistently, LAPTM4B interacts with Hrs in co-IP (Fig 6E) and colocalizes with Hrs at endosomes (Supplementary Fig S5B). Overexpression of the 6RQ mutant that lacks phosphoinositide binding further enhanced Hrs ubiquitination (Fig 6C and D). These results indicate that LAPTM4B interacts with Hrs, promoting Hrs ubiquitination, and that this role is inhibited by LAPTM4B phosphoinositide binding. Consistently, loss of PIPKIγi5 also promotes Hrs ubiquitination and diminished the Hrs interaction with EGFR (Sun *et al*, 2013b).

Nedd4, an E3 ubiquitin ligase that ubiquitinates Hrs, directly interacts with LAPTM4B (Katz *et al*, 2002; Persaud *et al*, 2009; Milkereit & Rotin, 2011). LAPTM4B and Nedd4 interact in both the endogenous and overexpressed conditions (Supplementary Fig S5C). We then examined whether LAPTM4B regulates Nedd4 interaction with Hrs. As shown in Fig 6F, overexpression of LAPTM4B enhanced Hrs association with Nedd4. Consistently, the 6RQ LAPTM4B mutant had increased interaction with Hrs compared to wild-type LAPTM4B (Fig 6E), and it also further enhanced the Nedd4–Hrs interaction (Fig 6F).

To investigate how phosphoinositide binding regulates the role of LAPTM4B in EGFR degradation, we used a lentivirus-based system to modestly overexpress LAPTM4B or the 6RQ mutant in cells. As shown in Fig 6G, the wild-type and 6RQ mutant of LAPTM4B were expressed at comparable levels. Wild-type LAPTM4B overexpression modestly inhibited EGFR degradation and enhanced AKT activation. The LAPTM4B 6RQ mutant overexpression showed enhanced inhibition of EGFR degradation and this resulted in enhanced AKT activation (Fig 6G and H). These data indicate that phosphoinositide binding relieves LAPTM4B inhibition of EGFR degradation.

LAPTM4B interacts with Nedd4 through two PY motifs (L/PPXY) at the LAPTM4B C-tail (Milkereit & Rotin, 2011). To confirm that Nedd4 interaction is required for LAPTM4B to inhibit EGFR degradation, the Nedd4-non-interacting LAPTM4B mutant (2PA) was generated in which the second conserved proline residues in both PY motifs were mutated into alanines. The 2PA mutant lost Nedd4 interaction but retained association with Hrs and had enhanced PIPKIγi5 interaction (Fig 6I). When comparing two pools of cells overexpressing high levels of LAPTM4B-WT or LAPT M4B-2PA, EGFR degradation was strongly inhibited in LAP TM4B-WT-expressing cells, but not in LAPTM4B-2PA cells (Fig 6J and K). This supports a role for the LAPTM4B–Nedd4 interaction in mediating inhibition of EGFR degradation.

PIPKIγi5 recruits SNX5 to inhibit LAPTM4B association with Hrs

We have previously shown that PIPKIγi5 C-tail also specifically interacts with SNX5 and controls SNX5 function in protecting Hrs from ubiquitination by Nedd4 (Sun *et al*, 2013b). As LAPTM4B and SNX5 both bind the PIPKIγi5 C-tail, we investigated whether they bind the same or distinct regions of the C-tail. A series of PIPKIγi5 C-terminal deletion mutants were generated and used for co-IP assays with LAPTM4B and SNX5. This revealed that the most N-terminus of the C-tail (amino acids 640-652) was required for SNX5 interaction, while the remaining C-terminus was not required (Fig 7A). In contrast, the LAPTM4B interaction with PIPKIγi5 required the full-length C-tail of

Figure 6. Phosphoinositide binding inhibits LAPTM4B interaction with Hrs and compromise the inhibitory effects of LAPTM4B in EGF-stimulated EGFR degradation.

A Control or LAPTM4B knockdown MDA-MB-231 cells were starved and stimulated with 100 ng/ml EGF for 30 min, and whole-cell lysates were subject to co-immunoprecipitation (co-IP) assay.

B Control or LAPTM4B knockdown MDA-MB-231 cells were transfected with His-tagged ubiquitin, starved, and stimulated with 100 ng/ml EGF for 30 min. Total ubiquitinated proteins were purified from whole-cell lysates by Ni-NTA agarose and analyzed by Western blot.

C Control or LAPTM4B-WT/6RQ-overexpressing MDA-MB-231 cells were transfected with His-tagged ubiquitin and myc-tagged Hrs, starved, and stimulated with 100 ng/ml EGF for 30 min before whole-cell lysate harvest. Total ubiquitinated proteins were purified by Ni-NTA agarose and analyzed by Western blot.

D Quantification of Hrs ubiquitination levels from the Western blot in (C) (mean + SD; $n = 5$).

E The co-IP of Myc-Hrs with Flag-LAPTM4B-WT or 6RQ mutant in HEK293 cells.

F The co-IP between Hrs and Nedd4 with Flag-LAPTM4B-WT or 6RQ mutant overexpression in HEK293 cells.

G The effects of LAPTM4B-6RQ mutant overexpression on EGF-stimulated EGFR degradation and signaling. Flag-LAPTM4B-WT or 6RQ mutant overexpression was accomplished by lentivirus-mediated infection approach. Cells with low levels of expression were selected as polyclonal pools for comparison. Control or overexpressing cells were starved and stimulated with 100 ng/ml EGF for indicated time periods and whole-cell lysates were analyzed by Western blot.

H Quantification of EGFR and pAKT levels from the Western blot in (G) (mean ± SD; $n = 5$).

I The PY motif mutant LAPTM4B-2PA loses interaction with Nedd4 but keeps interaction with Hrs in HEK293 cells cotransfected with the indicated proteins.

J The effects of LAPTM4B-2PA mutant overexpression on EGF-stimulated EGFR degradation and signaling. Overexpression of Flag-LAPTM4B-WT or 2PA mutant overexpression was accomplished by lentivirus-mediated infection approach. Cells with high expression of Flag-LAPTM4B were selected as polyclonal pools for comparison. Cells were starved and stimulated with 100 ng/ml EGF for the indicated time periods, and whole-cell lysates were analyzed by Western blot.

K Quantification of EGFR degradation from Western blot in (J) (mean ± SD; $n = 3$).

Data information: Data are representative from at least three independent experiments. L4B, LAPTM4B; Ub, ubiquitin; EV, empty vector.
Source data are available online for this figure.

PIPKIγi5 and deletion of 6 amino acids at the C-terminus diminished LAPTM4B interaction (Fig 7B and C). These data indicate that LAPTM4B and SNX5 may associate together with PIPKIγi5 on the C-tail. To test whether the PIPKIγi5 interactions integrate LAPTM4B and SNX5 into the same complex, a co-IP experiment was performed with or without PIPKIγi5 overexpression. This indicted that PIPKIγi5

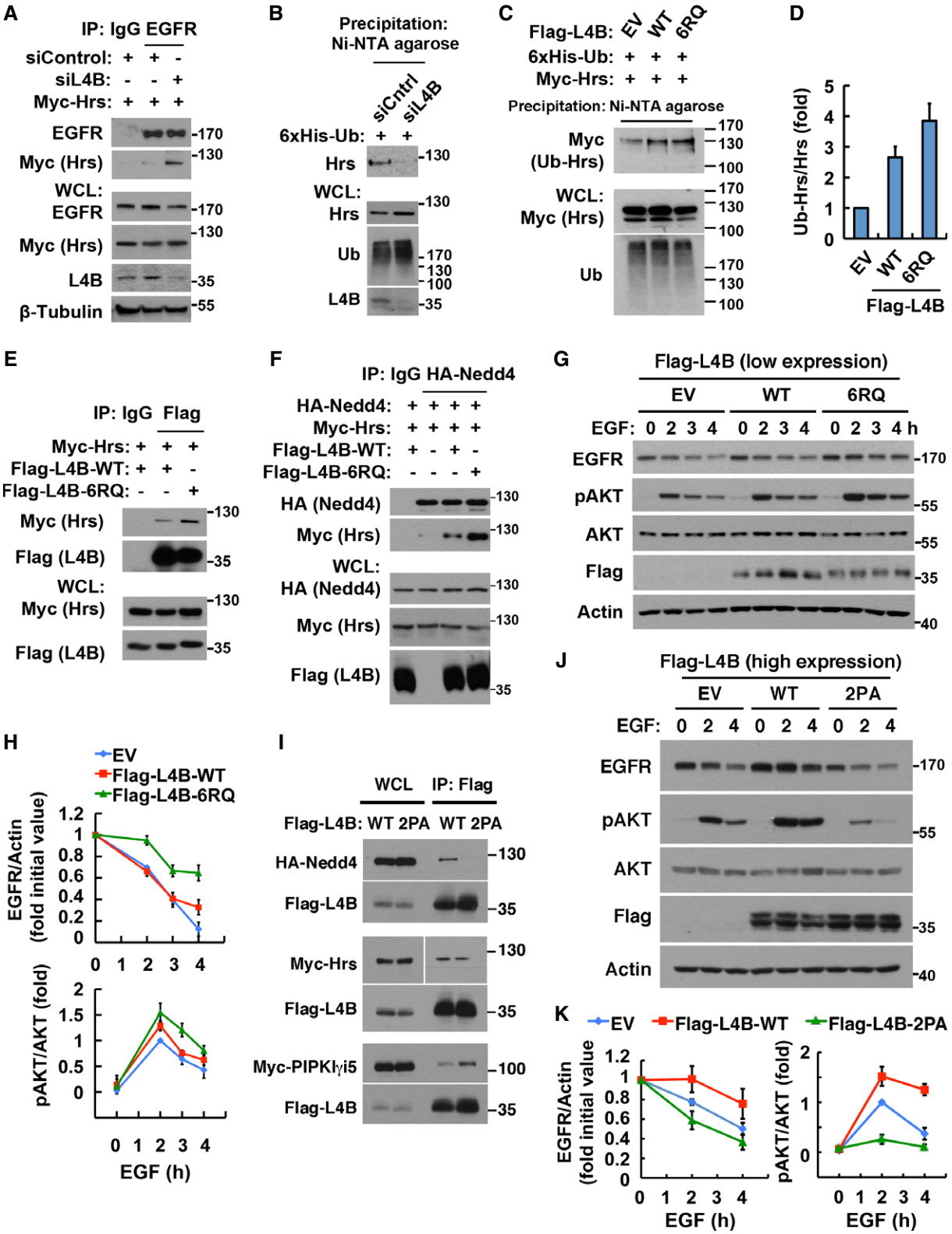

Figure 6.

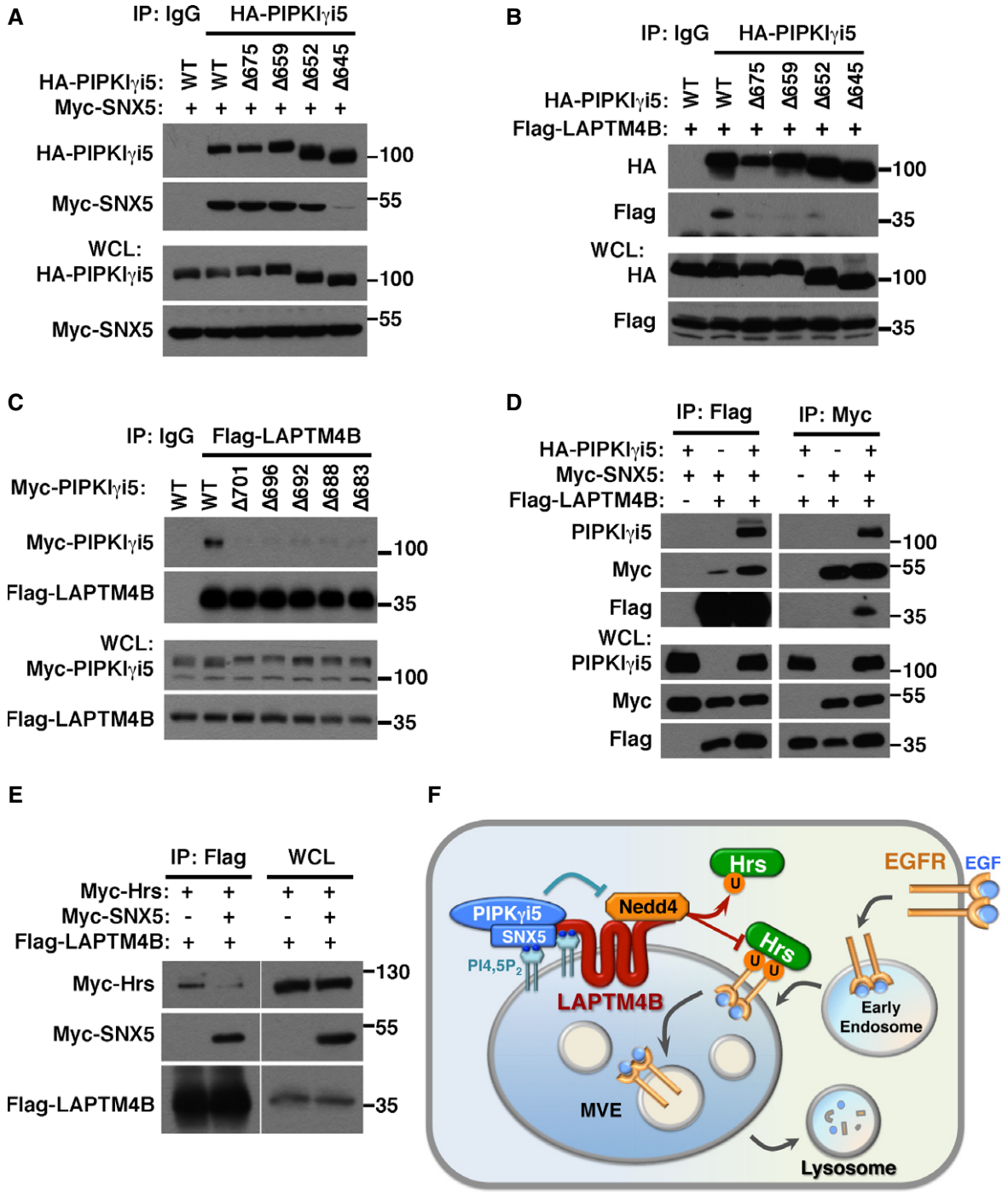

Figure 7. PIPKIγi5 recruits SNX5 to inhibit LAPTM4B association with Hrs.

A–C Co-immunoprecipitation (co-IP) of wild-type (WT) or C-terminal deletion mutants of HA-PIPKIγi5 with SNX5 (A) or LAPTM4B (B and C) in HEK293 cells cotransfected with indicated proteins. Δ675 indicates a deletion from amino acid 675 to the C-terminus.

D PIPKIγi5 promotes SNX5 association with LAPTM4B. HEK293 cells cotransfected with indicated proteins were harvested for co-IP to assay the interaction between Myc-SNX5 and Flag-LAPTM4B.

E SNX5 inhibits Hrs association with LAPTM4B. HEK293 cells cotransfected with indicated proteins were harvested for co-IP to assay the interaction between Myc-Hrs and Flag-LAPTM4B.

F A model for the PIPKIγi5–LAPTM4B pathway in EGFR trafficking. Hrs is an established key regulator of EGFR intraluminal sorting. LAPTM4B, by promoting Nedd4-mediated Hrs ubiquitination, inhibits the recognition of ubiquitinated EGFR by Hrs and therefore inhibits EGFR intraluminal sorting and lysosomal degradation. PIPKIγi5 directly binds to LAPTM4B and antagonizes the function of LAPTM4B in EGFR sorting by generating PtdIns(4,5)P_2 signals and recruiting SNX5.

Data information: Data are representative from at least three independent experiments.
Source data are available online for this figure.

strongly enhanced SNX5 association with LAPTM4B (Fig 7D). As SNX5 blocks Nedd4 interaction with Hrs (Sun *et al*, 2013b), we assessed whether SNX5 also inhibits LAPTM4B interaction with Nedd4 or Hrs. Overexpression of SNX5 suppressed LAPTM4B association with Hrs (Fig 7E), but not Nedd4 (Supplementary Fig S6A).

The data indicate a model where LAPTM4B inhibits Hrs-mediated EGFR degradation by promoting Hrs ubiquitination by Nedd4 (Fig 7F). To assess whether EGFR is selectively regulated by LAPTM4B, the consequence of LAPTM4B overexpression on the degradation of other receptors was examined. Neither hepatocyte growth factor (HGF)-induced degradation of c-Met nor SFLLRN-induced degradation of the G protein-coupled receptor PAR1 was inhibited by LAPTM4B overexpression (Supplementary Fig S6B–E). PAR1 degradation was accelerated in LAPTM4B-overexpressing cells. This indicates that LAPTM4B overexpression does not cause a general dysfunction of the lysosome or regulate the degradation of all receptors in the lysosome. These results are consistent with reports that Hrs is not essential for the degradation of c-Met or PAR1 (Gullapalli *et al*, 2006; Dores *et al*, 2012; Sun *et al*, 2013b), and suggest that LAPTM4B is selective for a subset of receptors sorted through Hrs.

Discussion

Agonist-activated cell surface receptors continue to signal through the endosomal pathways after internalization, and sorting to ILVs is required for signal termination of many receptors (Katzmann *et al*, 2002; Raiborg *et al*, 2003; McCullough *et al*, 2013). Intraluminal sorting followed by degradation in the lysosome downregulates EGFR. LAPTM4B is an endosomal tetra-transmembrane protein that is overexpressed in most epithelial cancers, induces transformation and tumorigenesis of normal human cells, correlates with poor prognosis in a number of cancers, and is linked to chemotherapy resistance and recurrence of breast cancer (Kasper *et al*, 2005; Li *et al*, 2010b, 2011; Yang *et al*, 2010b). Here, we show that LAPTM4B enhances EGFR signaling by blocking EGF-stimulated EGFR intraluminal sorting and degradation. In this pathway, LAPTM4B promotes Hrs ubiquitination, which blocks the recognition of ubiquitinated EGFR by Hrs (Fig 7). These results establish a key mechanism by which the known oncoprotein LAPTM4B facilitates pro-survival signaling in cancers. Consistently, cells with higher LAPTM4B expression are more proliferative and migratory (Yang *et al*, 2010a; Li *et al*, 2011), and this may explain why overexpression of LAPTM4B in cancers correlates with poor prognosis.

Intraluminal sorting is a highly conserved biological process that has been extensively studied over the past decade. The crystal structures of multiple ESCRT subunits have been solved resulting in detailed models of how ESCRT subunits could be recruited to endosomes and sort receptor cargos onto the ILVs (Williams & Urbé, 2007; Raiborg & Stenmark, 2009; Hurley, 2010). The ESCRT-related ILV sorting components so far identified are all cytosolic proteins, the functions of which require their recruitment to endosomes (Henne *et al*, 2011). LAPTM4B is an example of an endosomal resident transmembrane protein with a role in the intraluminal sorting of EGFR. While other studies reported a block of EGFR trafficking at early endosomes upon dysfunction of early ESCRT subunits, we observed that LAPTM4B regulates EGFR sorting at LAPTM4B-positive endosomes, primarily MVEs/late endosomes (Figs 3 and 4). This is due to inhibition of Hrs function at LAPTM4B-positive MVEs (Supplementary Fig S5B) and explains why LAPTM4B-expressing cells show enhanced EGFR–LAMP1 colocalization in the absence of lysosome inhibitor as this reflects a block at MVEs. The results demonstrate that LAPTM4B binds PIPKIγi5 and is a PtdIns(4,5)P_2 effector. PIPKIγi5 and its product PtdIns(4,5)P_2 are required for EGFR intraluminal sorting (Sun *et al*, 2013b), but LAPTM4B inhibits this pathway, indicating that LAPTM4B adds a layer of control to EGFR signaling by controlling sorting to ILVs and EGFR degradation. Our results demonstrate an additional layer of control regulated by the unexpected role of PtdIns(4,5)P_2 in endosome sorting (Sun *et al*, 2013b). LAPTM4B is a phosphoinositide-modulated resident endosomal transmembrane protein that may represent a protein family that functions to regulate receptor sorting by integrating with the ESCRT complexes that are recruited to endosomal surfaces.

The current understanding of ILV sorting is largely based on studies in yeast as most ESCRT subunits are conserved throughout evolution (Henne *et al*, 2011). Mammalian cells have evolved more complex ILV sorting systems that are less well defined. Our results expanded the understanding of the layer of regulation for EGFR ILV sorting in mammalian cells controlled by the PIPKIγi5–LAPTM4B interaction that is not conserved to yeast. The pro-survival role for human LAPTM4B depends on its N-tail (Shao *et al*, 2003), further emphasizing the importance of the LAPTM4B–PIPKIγi5 nexus in controlling EGFR signaling.

Though the majority of PtdIns(4,5)P_2 is localized at the plasma membrane (Watt *et al*, 2002; Sun *et al*, 2013c), PtdIns(4,5)P_2 is also observed at the endosomal limiting membrane, ILVs, and lysosomes (Arneson *et al*, 1999; Watt *et al*, 2002; Vicinanza *et al*, 2011; Rong *et al*, 2012; Shi *et al*, 2012). A number of PtdIns(4,5)P_2 binding proteins including SNX5, SNX9, adaptor protein 3 (AP3), and a group of Arf-GAPs were found to regulate endosomal trafficking (Vicinanza *et al*, 2008). Endosomal PIPKIγi5 and its kinase activity modulate the function of SNX5, a PtdIns(4,5)P_2 and PI3P effector, in EGFR endosomal sorting (Sun *et al*, 2013b). Consistently, depletion or accumulation of PtdIns(4,5)P_2 at endosomes have been reported to impact EGFR sorting and degradation (Ramel *et al*, 2011; Vicinanza *et al*, 2011). Although LAPTM4B binds multiple phosphoinositides *in vitro*, yet its interaction with PIPKIγi5 combined with its membrane topography indicates that it is an effector of PtdIns(4,5)P_2 (Fig 7F). In contrast to SNX5, also a PtdIns(4,5)P_2 effector, LAPTM4B acts as an inhibitor of the ESCRT-mediated EGFR degradation, and PtdIns(4,5)P_2 binding diminishes its inhibitory role. Interestingly, while endogenous LAPTM4B is localized to both early and late endosomes, LAPTM4B regulates EGFR trafficking primarily at the late endosome, possibly due to inhibition of LAPTM4B functions by PIPKIγi5, PtdIns(4,5)P_2, and SNX5 at early endosomes. The results indicate that generation of PtdIns(4,5)P_2 modulates the interactions between SNX5, LAPTM4B, the ESCRT-0 subunit Hrs, and the E3 ubiquitin ligase Nedd4. This regulates the interaction of Nedd4 with its substrate Hrs. The ubiquitination of Hrs in turn controls its interaction with EGFR and subsequent ILV sorting of EGFR. LAPTM4B has two PY motifs, while Hrs has only one. LAPTM4B may interact with Nedd4 and orient it with Hrs so that Hrs is a better Nedd4 substrate, suggesting that LAPTM4B has a scaffold function that regulates Nedd4 activity toward Hrs. The LAPTM4B complex with PIPKIγi5 also suggests that

it may regulate Nedd4 specificity toward other substrates in addition to Hrs.

Epidermal growth factor receptor and hundreds of other receptors are downregulated by ILV sorting and lysosomal degradation (Raiborg & Stenmark, 2009; Sorkin & von Zastrow, 2009), suggesting that there is receptor specificity for sorting and degradation. LAPTM4B is a selective regulator for EGFR trafficking, as it does not inhibit degradation of c-Met or PAR1 (Supplementary Fig S6B–E). PIPKIγi5 and SNX5 also selectively regulate the degradation of EGFR (Sun *et al*, 2013b). The role of PIPKIγi5, PtdIns(4,5)P_2, SNX5, and LAPTM4B putatively defines a pathway for selective and regulated sorting and destruction of receptors. The receptor preference for different ESCRT subunits and the cross talks between ESCRT complexes and LAPTM proteins as well as other endosomal transmembrane proteins including the tetraspanin family members may modulate this specificity.

Overexpression of LAPTM4B has been shown to enhance chemotherapy resistance in cancer cells, and this was associated with AKT activation (Li *et al*, 2010a,b). Phosphorylated AKT is a known locus for cancer multi-drug resistance (Radisavljevic, 2013). Our study indicates that LAPTM4B promotes AKT signaling by blocking EGFR degradation and this would be one mechanism for the role of LAPTM4B in drug resistance. The combined information suggests that LAPTM4B could be a potential therapeutic target for cancers that are addicted to EGFR signaling or in circumstances where chemotherapy resistance occurs.

Materials and Methods

Reagents, constructs, and cells

A detailed description of reagents, constructs, and cell treatment is included in Supplementary Materials and Methods. MDA-MB-231 and HEK293 cells were cultured in DMEM supplemented with 10% FBS. Transfection of plasmids and siRNA oligonucleotides was carried out using Lipofectamine 2000 and Oligofectamine (Invitrogen, Carlsbad, CA, USA), respectively, according to manufacturer's instructions.

Immunofluorescence microscopy

Cells on glass coverslips were washed with PBS, fixed in 4% paraformaldehyde (PFA), and permeabilized in 0.5% Triton X-100 in PBS for 10 min, followed by blocking in 3% BSA for 1 h at room temperature. Incubation with primary antibodies was performed at 37°C for 2 h or 4°C overnight. Then cells were washed twice in washing buffer (0.1% Triton X-100 in PBS) and incubated with secondary antibodies at room temperature for 30–60 min, followed by washing three times with washing buffer. Fluorescence images were obtained using MetaMorph with Nikon Eclipse TE2000-U microscope and further processed in MetaMorph. For colocalization quantification, images were background-subtracted and split into individual channels (e.g. channel 1 for EGFR; channel 2 for EEA1), and the colocalization quantification of signals from two individual channels was performed using the Coloc 2 plugin of Fiji (ImageJ). The thresholded Manders M1 coefficient was expressed as percentages (e.g. M1 = 0.3 was expressed as 30%) to show the fraction of intensities in channel 1 above threshold that is colocalized with intensities in channel 2 above threshold.

Electron microscopy

For EGFR intraluminal sorting, control or LAPTM4B knockdown cells were starved, labeled with anti-EGFR, followed by protein A-gold labeling. Cells were then stimulated with EGF for 1 h at 37°C, fixed with 2% glutaraldehyde in 0.1 M sodium phosphate buffer (PB), and processed for EM examination in UW Medical School EM facility. See Supplementary Materials and Methods for more details.

The specific localizations of LAPTM4B at endosomes were detected by silver-enhanced immuno-EM. Briefly, cells were fixed with 0.1% glutaraldehyde and 2% paraformaldehyde, permeabilized with 0.1% Triton X-100 for 30 min, blocked in Aurion blocking solution for 1 h, followed by another 1 h of blocking with incubation buffer. Cells were then stained with LAPTM4B anti-sera, washed and incubated with ultra-small gold-conjugated goat anti-rabbit IgG overnight at 4°C. Cell were washed and post-fixed with 2% glutaraldehyde and then silver-enhanced. Ultra-thin sections were examined as described above. See Supplementary Materials and Methods for more details.

Alexa-555-EGF degradation assays

MDA-MB-231 cells transfected with control or LAPTM4B siRNA were re-plated on to cover slips 48 h after transfection. Cells were starved for 3 h and pulsed with 25 ng/ml Alexa-555-EGF for 3 min, and unbound EGF washed out by changing medium twice. Cells were fixed at indicated time points after Alexa-555-EGF stimulation. Fixed cells were incubated with DAPI for 2 min and washed three times with washing buffer. The total amount of Alexa-555-EGF fluorescence was quantified in Fiji, and the cell number on each image was counted using the nucleus (DAPI) staining as a reference. The average amount of Alexa-555-EGF per cell was calculated by dividing the total amount of Alexa-555-EGF fluorescence by the total cell number.

Intraluminal sorting of EGF

MDA-MB-231 cells on coverslips were transfected with EGFP-Rab5Q79L, starved for 4 h, and stimulated with 100 ng/ml Alexa-555-EGF for indicated time periods, followed by fixation in 4% PFA before fluorescence microscopy. Quantification of EGF on the limiting membrane and within the endosomal lumen was done as described (Trajkovic *et al*, 2008). Briefly, central images of endosomes (diameter > 2 μm) were taken with the GFP-Rab5Q79L outline as a reference. For quantification, the GFP-Rab5Q79L outline was also used as a reference to determine the EGF localization on the limiting membrane. EGF localized inside the GFP-Rab5Q79L outline was considered as intraluminal EGF. The total intensities of endosomal EGF fluorescence and the intensities inside the GFP-Rab5Q79L outline were quantified using Fiji. Calculation of significance is made by Student's *t*-test.

Supplementary information for this article is available online: http://emboj.embopress.org

Acknowledgments

We thank Drs Suyong Choi, Rakesh Singh, and Weimin Li for discussions. We thank SJ Parsons (University of Virginia) for the EGFR-K721A construct, R Zhou (Peking University) for LAPTM4B construct, R Puertollano (National Institutes of Health) for the LAPTM4A construct, and W Yang (Geisinger Clinic) for the Nedd4 constructs. This work is supported by National Institute of Health Grants CA104708 and GM057549 to R.A.A., Howard Hughes Medical Institute International Student Research Fellowship to X.T., American Heart Association Scientist Development Grant 12SDG11950022 to Y.S., American Heart Association Postdoctoral Fellowship (10POST4290052) to N.T., and Hilldale Undergraduate/Faculty Research Fellowship to Y.L.

Author contributions

XT and RAA conceived the study. XT, YS, ACH, and RAA designed experiments. XT, YS, YL, and NT performed experiments. XT, YS, ACH, and RAA analyzed data. XT and RAA wrote the manuscript.

Conflict of interest

The authors declare that they have no conflict of interest.

References

Adra C, Zhu S, Ko J, Guillemot J, Cuervo A, Kobayashi H, Horiuchi T, Lelias J, Rowley J, Lim B (1996) LAPTM5: a novel lysosomal-associated multispanning membrane protein preferentially expressed in hematopoietic cells. *Genomics* 35: 328 – 337

Anderson RA, Marchesi VT (1985) Regulation of the association of membrane skeletal protein 4.1 with glycophorin by a polyphosphoinositide. *Nature* 318: 295 – 298

Arneson L, Kunz J, Anderson R, Traub L (1999) Coupled inositide phosphorylation and phospholipase D activation initiates clathrin-coat assembly on lysosomes. *J Biol Chem* 274: 17794 – 17805

Bairstow SF, Ling K, Su X, Firestone AJ, Carbonara C, Anderson RA (2006) Type Igamma 661 phosphatidylinositol phosphate kinase directly interacts with AP2 and regulates endocytosis. *J Biol Chem* 281: 20632 – 20642

Balla T (2013) Phosphoinositides: tiny lipids with giant impact on cell regulation. *Physiol Rev* 93: 1019 – 1137

Di Paolo G, De Camilli P (2006) Phosphoinositides in cell regulation and membrane dynamics. *Nature* 443: 651 – 657

Dores MR, Chen B, Lin H, Soh UJ, Paing MM, Montagne WA, Meerloo T, Trejo J (2012) ALIX binds a YPX(3)L motif of the GPCR PAR1 and mediates ubiquitin-independent ESCRT-III/MVB sorting. *J Cell Biol* 197: 407 – 419

Eden ER, Huang F, Sorkin A, Futter CE (2012) The role of EGF receptor ubiquitination in regulating its intracellular traffic. *Traffic* 13: 329 – 337

Eden ER, White IJ, Futter CE (2009) Down-regulation of epidermal growth factor receptor signalling within multivesicular bodies. *Biochem Soc Trans* 37(Pt 1): 173 – 177

Eguchi S, Frank G, Mifune M, Inagami T (2003) Metalloprotease-dependent ErbB ligand shedding in mediating EGFR transactivation and vascular remodelling. *Biochem Soc Trans* 31(Pt 6): 1198 – 1202

Gullapalli A, Wolfe BL, Griffin CT, Magnuson T, Trejo J (2006) An essential role for SNX1 in lysosomal sorting of protease-activated receptor-1: evidence for retromer-, Hrs-, and Tsg101-independent functions of sorting nexins. *Mol Biol Cell* 17: 1228 – 1238

Hanafusa H, Ishikawa K, Kedashiro S, Saigo T, Iemura S, Natsume T, Komada M, Shibuya H, Nara A, Matsumoto K (2011) Leucine-rich repeat kinase LRRK1 regulates endosomal trafficking of the EGF receptor. *Nat Commun* 2: 158

Heck JN, Mellman DL, Ling K, Sun Y, Wagoner MP, Schill NJ, Anderson RA (2007) A conspicuous connection: structure defines function for the phosphatidylinositol-phosphate kinase family. *Crit Rev Biochem Mol Biol* 42: 15 – 39

Henne WM, Buchkovich NJ, Emr SD (2011) The ESCRT pathway. *Dev Cell* 21: 77 – 91

Henne WM, Stenmark H, Emr SD (2013) Molecular mechanisms of the membrane sculpting ESCRT pathway. *Cold Spring Harb Perspect Biol* 5: a016766

Hoeller D, Crosetto N, Blagoev B, Raiborg C, Tikkanen R, Wagner S, Kowanetz K, Breitling R, Mann M, Stenmark H, Dikic I (2006) Regulation of ubiquitin-binding proteins by monoubiquitination. *Nat Cell Biol* 8: 163 – 169

Hogue D, Nash C, Ling V, Hobman T (2002) Lysosome-associated protein transmembrane 4 alpha (LAPTM4 alpha) requires two tandemly arranged tyrosine-based signals for sorting to lysosomes. *Biochem J* 365(Pt 3): 721 – 730

Huang C (2007) Complex roles of PIP2 in the regulation of ion channels and transporters. *Am J Physiol Renal Physiol* 293: F1761 – F1765

Hurley JH (2010) The ESCRT complexes. *Crit Rev Biochem Mol Biol* 45: 463 – 487

Kagiyama S, Eguchi S, Frank G, Inagami T, Zhang Y, Phillips M (2002) Angiotensin II-induced cardiac hypertrophy and hypertension are attenuated by epidermal growth factor receptor antisense. *Circulation* 106: 909 – 912

Kang Y, Yin M, Jiang W, Zhang H, Xia B, Xue Y, Huang Y (2012) Overexpression of LAPTM4B-35 is associated with poor prognosis in colorectal carcinoma. *Am J Surg* 204: 677 – 683

Kasper G, Vogel A, Klaman I, Gröne J, Petersen I, Weber B, Castaños-Vélez E, Staub E, Mennerich D (2005) The human LAPTM4b transcript is upregulated in various types of solid tumours and seems to play a dual functional role during tumour progression. *Cancer Lett* 224: 93 – 103

Katz M, Shtiegman K, Tal-Or P, Yakir L, Mosesson Y, Harari D, Machluf Y, Asao H, Jovin T, Sugamura K, Yarden Y (2002) Ligand-independent degradation of epidermal growth factor receptor involves receptor ubiquitylation and Hgs, an adaptor whose ubiquitin-interacting motif targets ubiquitylation by Nedd4. *Traffic* 3: 740 – 751

Katzmann DJ, Odorizzi G, Emr SD (2002) Receptor downregulation and multivesicular-body sorting. *Nat Rev Mol Cell Biol* 3: 893 – 905

Li L, Shan Y, Yang H, Zhang S, Lin M, Zhu P, Chen XY, Yi J, McNutt MA, Shao GZ, Zhou RL (2011) Upregulation of LAPTM4B-35 promotes malignant transformation and tumorigenesis in L02 human liver cell line. *Anat Rec (Hoboken)* 294: 1135 – 1142

Li L, Wei XH, Pan YP, Li HC, Yang H, He QH, Pang Y, Shan Y, Xiong FX, Shao GZ, Zhou RL (2010a) LAPTM4B: a novel cancer-associated gene motivates multidrug resistance through efflux and activating PI3K/AKT signaling. *Oncogene* 29: 5785 – 5795

Li Y, Zou L, Li Q, Haibe-Kains B, Tian R, Li Y, Desmedt C, Sotiriou C, Szallasi Z, Iglehart JD, Richardson AL, Wang ZC (2010b) Amplification of LAPTM4B and YWHAZ contributes to chemotherapy resistance and recurrence of breast cancer. *Nat Med* 16: 214 – 218

Lindmo K, Stenmark H (2006) Regulation of membrane traffic by phosphoinositide 3-kinases. *J Cell Sci* 119(Pt 4): 605 – 614

Ling K, Doughman RL, Firestone AJ, Bunce MW, Anderson RA (2002) Type I gamma phosphatidylinositol phosphate kinase targets and regulates focal adhesions. *Nature* 420: 89 – 93

McCullough J, Colf LA, Sundquist WI (2013) Membrane Fission Reactions of the Mammalian ESCRT Pathway. *Annu Rev Biochem* 82: 663 – 692

Mellman D, Gonzales M, Song C, Barlow C, Wang P, Kendziorski C, Anderson R (2008) A PtdIns4,5P2-regulated nuclear poly(A) polymerase controls expression of select mRNAs. *Nature* 451: 1013 – 1017

Mendelsohn J, Baselga J (2006) Epidermal growth factor receptor targeting in cancer. *Semin Oncol* 33: 369 – 385

Milkereit R, Rotin D (2011) A role for the ubiquitin ligase Nedd4 in membrane sorting of LAPTM4 proteins. *PLoS ONE* 6: e27478

Pak Y, Glowacka W, Bruce M, Pham N, Rotin D (2006) Transport of LAPTM5 to lysosomes requires association with the ubiquitin ligase Nedd4, but not LAPTM5 ubiquitination. *J Cell Biol* 175: 631 – 645

Persaud A, Alberts P, Amsen E, Xiong X, Wasmuth J, Saadon Z, Fladd C, Parkinson J, Rotin D (2009) Comparison of substrate specificity of the ubiquitin ligases Nedd4 and Nedd4-2 using proteome arrays. *Mol Syst Biol* 5: 333

Radisavljevic Z (2013) AKT as locus of cancer multidrug resistance and fragility. *J Cell Physiol* 288: 671 – 674

Raiborg C, Bache K, Gillooly D, Madshus I, Stang E, Stenmark H (2002) Hrs sorts ubiquitinated proteins into clathrin-coated microdomains of early endosomes. *Nat Cell Biol* 4: 394 – 398

Raiborg C, Rusten TE, Stenmark H (2003) Protein sorting into multivesicular endosomes. *Curr Opin Cell Biol* 15: 446 – 455

Raiborg C, Stenmark H (2009) The ESCRT machinery in endosomal sorting of ubiquitylated membrane proteins. *Nature* 458: 445 – 452

Ramel D, Lagarrigue F, Pons V, Mounier J, Dupuis-Coronas S, Chicanne G, Sansonetti PJ, Gaits-Iacovoni F, Tronchere H, Payrastre B (2011) Shigella flexneri infection generates the lipid PI5P to alter endocytosis and prevent termination of EGFR signaling. *Sci Signal* 4: ra61

Rong Y, Liu M, Ma L, Du W, Zhang H, Tian Y, Cao Z, Li Y, Ren H, Zhang C, Li L, Chen S, Xi J, Yu L (2012) Clathrin and phosphatidylinositol-4,5-bisphosphate regulate autophagic lysosome reformation. *Nat Cell Biol* 14: 924 – 934

Schill N, Anderson R (2009) Two novel phosphatidylinositol-4-phosphate 5-kinase type Igamma splice variants expressed in human cells display distinctive cellular targeting. *Biochem J* 422: 473 – 482

Schramp M, Hedman A, Li W, Tan X, Anderson R (2012) PIP kinases from the cell membrane to the nucleus. *Subcell Biochem* 58: 25 – 59

Shao G, Zhou R, Zhang Q, Zhang Y, Liu J, Rui J, Wei X, Ye D (2003) Molecular cloning and characterization of LAPTM4B, a novel gene upregulated in hepatocellular carcinoma. *Oncogene* 22: 5060 – 5069

Shi A, Liu O, Koenig S, Banerjee R, Chen CC, Eimer S, Grant BD (2012) RAB-10-GTPase-mediated regulation of endosomal phosphatidylinositol-4,5-bisphosphate. *Proc Natl Acad Sci USA* 109: E2306 – E2315

Sigismund S, Argenzio E, Tosoni D, Cavallaro E, Polo S, Di Fiore P (2008) Clathrin-mediated internalization is essential for sustained EGFR signaling but dispensable for degradation. *Dev Cell* 15: 209 – 219

Simonsen A, Lippé R, Christoforidis S, Gaullier J, Brech A, Callaghan J, Toh B, Murphy C, Zerial M, Stenmark H (1998) EEA1 links PI(3)K function to Rab5 regulation of endosome fusion. *Nature* 394: 494 – 498

Sorkin A, Goh LK (2008) Endocytosis and intracellular trafficking of ErbBs. *Exp Cell Res* 314: 3093 – 3106

Sorkin A, Krolenko S, Kudrjavtceva N, Lazebnik J, Teslenko L, Soderquist AM, Nikolsky N (1991) Recycling of epidermal growth factor-receptor complexes in A431 cells: identification of dual pathways. *J Cell Biol* 112: 55 – 63

Sorkin A, von Zastrow M (2009) Endocytosis and signalling: intertwining molecular networks. *Nat Rev Mol Cell Biol* 10: 609 – 622

Stenmark H, Parton RG, Steele-Mortimer O, Lutcke A, Gruenberg J, Zerial M (1994) Inhibition of rab5 GTPase activity stimulates membrane fusion in endocytosis. *EMBO J* 13: 1287 – 1296

Suh B, Hille B (2005) Regulation of ion channels by phosphatidylinositol 4,5-bisphosphate. *Curr Opin Neurobiol* 15: 370 – 378

Sun Y, Hedman AC, Tan X, Anderson RA (2013a) An unexpected role for PI4,5P 2 in EGF receptor endosomal trafficking. *Cell Cycle* 12: 1991 – 1992

Sun Y, Hedman AC, Tan X, Schill NJ, Anderson RA (2013b) Endosomal type igamma PIP 5-kinase controls EGF receptor lysosomal sorting. *Dev Cell* 25: 144 – 155

Sun Y, Thapa N, Hedman AC, Anderson RA (2013c) Phosphatidylinositol 4,5-bisphosphate: targeted production and signaling. *BioEssays* 35: 513 – 522

Thapa N, Sun Y, Schramp M, Choi S, Ling K, Anderson RA (2012) Phosphoinositide signaling regulates the exocyst complex and polarized integrin trafficking in directionally migrating cells. *Dev Cell* 22: 116 – 130

Trajkovic K, Hsu C, Chiantia S, Rajendran L, Wenzel D, Wieland F, Schwille P, Brugger B, Simons M (2008) Ceramide triggers budding of exosome vesicles into multivesicular endosomes. *Science* 319: 1244 – 1247

Vergarajauregui S, Martina J, Puertollano R (2011) LAPTMs regulate lysosomal function and interact with mucolipin 1: new clues for understanding mucolipidosis type IV. *J Cell Sci* 124(Pt 3): 459 – 468

Vicinanza M, D'Angelo G, Di Campli A, De Matteis MA (2008) Function and dysfunction of the PI system in membrane trafficking. *EMBO J* 27: 2457 – 2470

Vicinanza M, Di Campli A, Polishchuk E, Santoro M, Di Tullio G, Godi A, Levtchenko E, De Leo MG, Polishchuk R, Sandoval L, Marzolo MP, De Matteis MA (2011) OCRL controls trafficking through early endosomes via PtdIns4,5P (2)-dependent regulation of endosomal actin. *EMBO J* 30: 4970 – 4985

Watt S, Kular G, Fleming I, Downes C, Lucocq J (2002) Subcellular localization of phosphatidylinositol 4,5-bisphosphate using the pleckstrin homology domain of phospholipase C delta1. *Biochem J* 363(Pt 3): 657 – 666

Wiley HS (2003) Trafficking of the ErbB receptors and its influence on signaling. *Exp Cell Res* 284: 78 – 88

Williams R, Urbé S (2007) The emerging shape of the ESCRT machinery. *Nat Rev Mol Cell Biol* 8: 355 – 368

Xia Y, Irvine RF, Giudici ML (2011) Phosphatidylinositol 4-phosphate 5-kinase Igamma_v6, a new splice variant found in rodents and humans. *Biochem Biophys Res Commun* 411: 416 – 420

Yang H, Xiong F, Wei X, Yang Y, McNutt M, Zhou R (2010a) Overexpression of LAPTM4B-35 promotes growth and metastasis of hepatocellular carcinoma in vitro and in vivo. *Cancer Lett* 294: 236 – 244

Yang H, Xiong FX, Lin M, Yang Y, Nie X, Zhou RL (2010b) LAPTM4B-35 overexpression is a risk factor for tumor recurrence and poor prognosis in hepatocellular carcinoma. *J Cancer Res Clin Oncol* 136: 275 – 281

